198585: pelitic gneiss, Griffins Find

(South West Terrane, Yilgarn Craton)

Blereau, ER, Korhonen, FJ, Fielding, IOH and Romano, SS

Location and sampling

DUMBLEYUNG (SI 50-7), KUKERIN (2531)

MGA Zone 50, 623327E 6340435N

Warox Site FJKBGD198585

Sampled on 7 June 2010

This sample was collected from a talus slope at the abandoned Griffins Find mine, about 13.8 km west-northwest of Lake Grace townsite, 13.5 km south-southwest of Carrajon farm, and 4.4 km north of the Dumbleyung – Lake Grace Road. The sample was collected as part of the Yilgarn Craton Metamorphic Project (2003–14) undertaken by Ben Goscombe for the Geological Survey of Western Australia (GSWA), and referred to in that study as sample BG10-39h. The results from this project have not been released by GSWA, although select data have been published in Goscombe et al. (2019).

Geological context

The unit sampled is a pelitic gneiss near the western margin of the Youanmi Terrane (Quentin de Gromard et al., 2021). This unit is part of a northwest-trending belt of Archean metasedimentary and gneissic rocks previously assigned to the South West Terrane and referred to informally by Wilde (2001) as the 'Lake Grace domain' (cf. Pidgeon et al., 2010). The boundary between the South West and Youanmi Terranes in this area is a major, northwest-trending shear zone system (Quentin de Gromard et al., 2021). Two samples of garnet-bearing alkali feldspar granite from Griffins Find yielded crystallization ages of c. 2636 Ma (Qiu and McNaughton, 1999). A quartzite also collected from Griffins Find yielded detrital zircon dates between c. 3812 and 2643 Ma, and a conservative maximum age of deposition of 2655 ± 11 Ma (GSWA 198580, Lu et al., 2015b). A pelitic gneiss from Griffins Find yielded detrital zircon dates between c. 2838 and 2629 Ma, and a conservative maximum depositional age of 2638 ± 2 Ma (GSWA 198578; Lu et al., 2015a). Monazite from the sample reported here yielded a weighted mean $^{207}Pb/^{206}Pb$ date of 2641 ± 6 Ma, interpreted as the age of high-grade metamorphism (GSWA 198585, Fielding et al., 2021).

Petrographic description

The sample is a weakly foliated, fine- to medium-grained pelitic gneiss, consisting of about 30% quartz, 28–30% cordierite, 18–20% garnet, 15% biotite, 4–5% orthopyroxene, 4–5% plagioclase, minor ilmenite and pyrrhotite, and trace pyrite, graphite, monazite and zircon (Fig. 1, Table 1). The matrix consists of mainly fine-grained (0.5 mm) granoblastic quartz intergrown with cordierite and platy red–brown biotite, together with subordinate orthopyroxene and plagioclase that define an anastomosing foliation that wraps garnet poikiloblasts. Quartz in the matrix is anhedral, 0.5 to 4 mm in size, and exhibits undulose extinction. Rare elongate grains of quartz and plagioclase, which are interpreted to represent former melt films, also occur on the margins of garnet porphyroblasts. Cordierite is anhedral, equant to slightly elongate, up to 2 mm in diameter, contains inclusions of quartz and biotite, and exhibits radiation halos from included accessory minerals (Figs 1, 2a). Garnet porphyroblasts are up to 4 mm in diameter and form equant anhedral poikiloblasts with cores containing abundant inclusions of rounded quartz, and minor biotite and ilmenite (Figs 1, 2). Rare cordierite inclusions occur within the rims of some garnet. Small rounded inclusions of relict garnet occur in cordierite (Fig. 2a), and less commonly in orthopyroxene. Garnet porphyroblasts are almandine-rich (X_{Alm} = 0.55, X_{Prp} = 0.38, X_{Grs} = 0.06) with weak compositional zoning (Appendix 1). There is a slight decrease in Ca contents from core to rim (X_{Grs} = 0.05), and rims adjacent to biotite show an increase in Fe contents (X_{Alm} = 0.64, X_{Prp} = 0.26, X_{Grs} = 0.05). Laths of red–orange biotite

up to 2 mm long define a weak, anastomosing foliation. Biotite envelops garnet and is intergrown with orthopyroxene, cordierite and quartz (Fig. 2). Coarse-grained orthopyroxene porphyroblasts up to 6 mm across are in direct contact with garnet (Fig. 2a), and show green to pale yellow pleochroism and first-order grey–yellow birefringence. Small rounded inclusions of relict garnet are present in some orthopyroxene porphyroblasts, but are not common. Finer grained orthopyroxene, up to 1 mm long, with pink–green pleochroism and second-order pink–orange birefringence occurs with cordierite, biotite(–plagioclase) and minor quartz in the matrix (Fig. 2b). Plagioclase is 0.5 to 1 mm in size, and occurs mainly with orthopyroxene and garnet, and less commonly with cordierite and quartz. Opaque minerals in the matrix are up to 0.5 mm in diameter, and are mainly ilmenite, pyrrhotite and pyrite. This granulite facies gneiss was likely derived from a pelitic metasedimentary protolith.

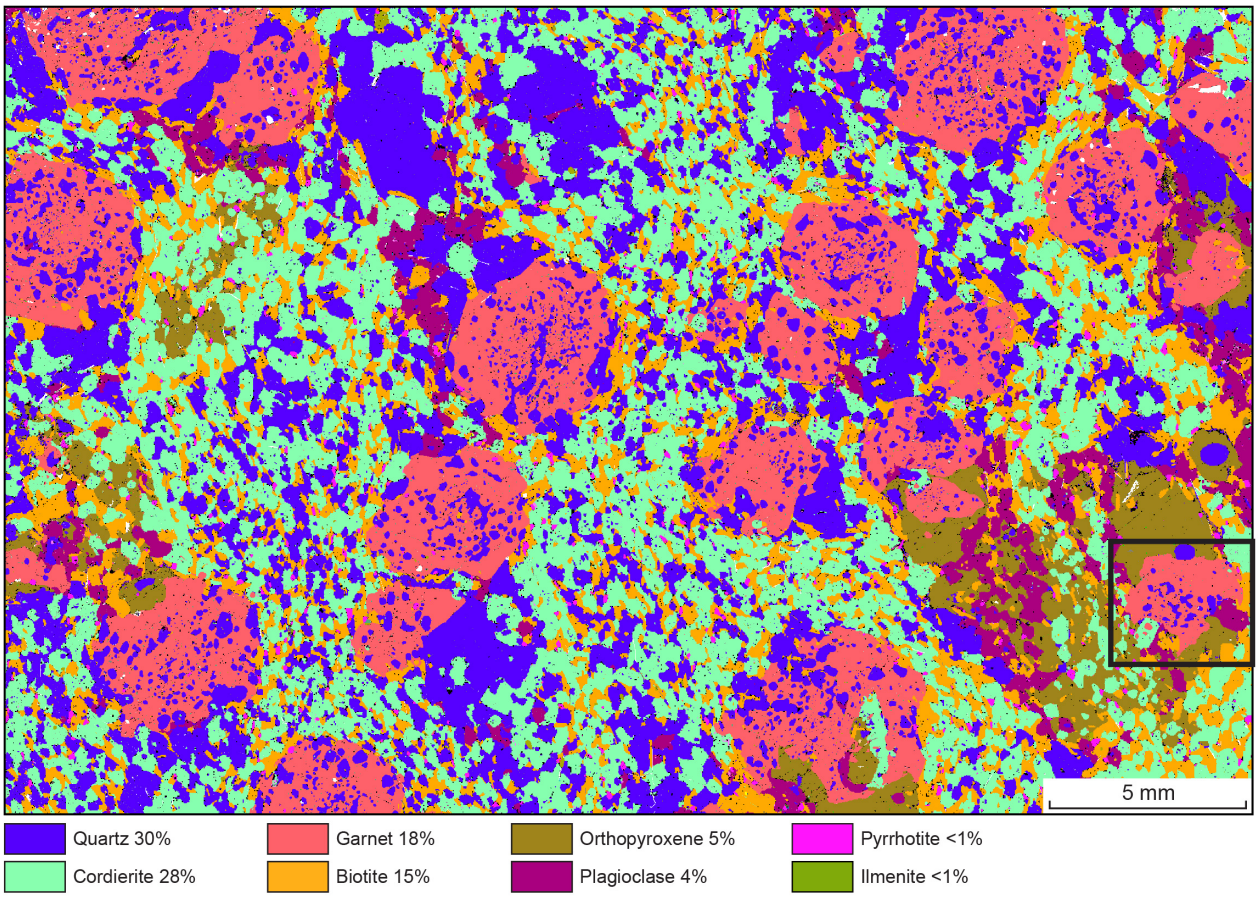

Figure 1. **TESCAN Integrated Mineral Analyser (TIMA) image of an entire thin section from sample 198585: pelitic gneiss, Griffins Find. Volume percent proportions of major rock-forming minerals are calculated by the TIMA software. Black rectangle shows location of electron probe micro-analyser (EPMA) garnet map (Appendix 1)**

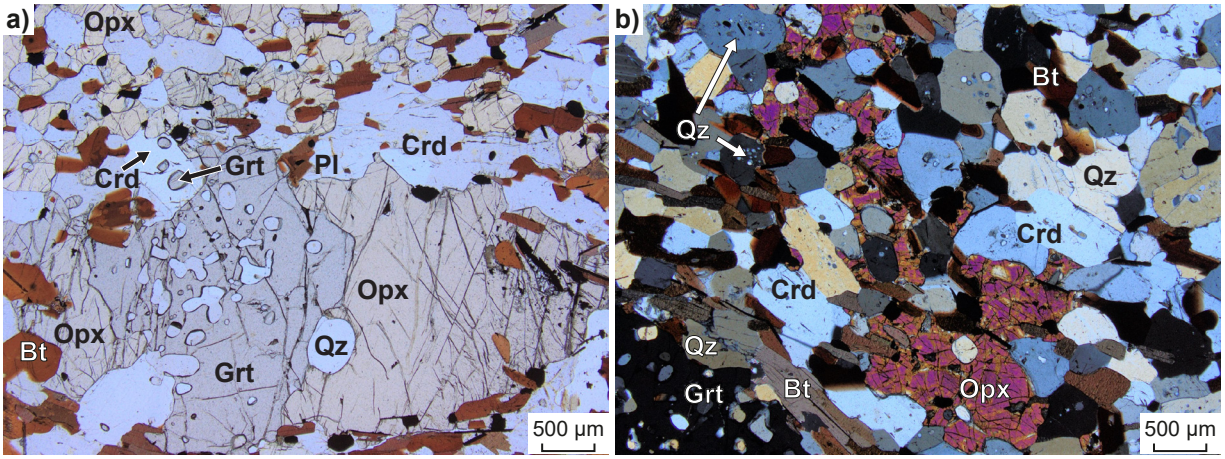

Figure 2. **Photomicrographs of sample 198585: pelitic gneiss, Griffins Find: a) plane-polarized light; b) cross-polarized light. Mineral abbreviations are explained in the caption to Figure 3**

Table 1. Mineral modes for sample 198585: pelitic gneiss, Griffins Find

Mineral modes	Grt	Opx	Crd	Bt	Kfs	Pl	Qz	Ilm	Liq
Observed (vol%)[a]	18	5	28	15[b]	–	4	30	minor	–
Predicted (mol%)									
@ 890 °C, 4.1 kbar	0.2	29	34	–	2	8	8	1	18
@ 890 °C, 6.2 kbar	45	2	11	–	3	4	17	1	16

NOTES: (a) Minor pyrrhotite, trace pyrite, graphite, monzite and zircon also present in thin section
(b) Intepreted as retrograde
– not present

Analytical details

Preliminary *P–T* estimates were obtained using multiple-reaction thermobarometry calculated from the mineral compositions (Table 2; Goscombe et al., 2019). These estimates were derived from the 'averagePT' module (avPT) in the program THERMOCALC version tc325 (Powell and Holland, 1988), using the internally consistent Holland and Powell (1998) dataset.

The metamorphic evolution of this sample was investigated using phase equilibria modelling, based on the bulk rock composition (Table 3). The bulk rock composition was determined by X-ray fluorescence spectroscopy, together with loss on ignition (LOI). FeO content was analysed by Fe^{2+} titration, and Fe_2O_3 calculated by difference. The modelled O content (for Fe^{3+}) was derived from the titration value; the modelled H_2O content was the measured LOI. The bulk composition was adjusted for the presence of apatite by applying a correction to CaO (Table 3). Thermodynamic calculations were performed in the MnNCKFMASHTO ($MnO–Na_2O–CaO–K_2O–FeO–MgO–Al_2O_3–SiO_2–H_2O–TiO_2–O$) system using THERMOCALC version tc340 (Powell and Holland, 1988; updated October 2013) and the internally consistent thermodynamic dataset of Holland and Powell (2011; dataset tc-ds62, created in February 2012). The activity–composition relations used in the modelling are detailed in White et al. (2014a,b). Compositional and mode isopleths for all phases were calculated using the software TCInvestigator (Pearce et al., 2015). Additional information on the workflow with relevant background and methodology are provided in Korhonen et al. (2020).

Table 2. Mineral compositions for sample 198585: pelitic gneiss, Griffins Find

Mineral[a]	Bt	Bt	Crd	Crd	Pl	Pl	Grt	Grt	Grt	Grt
Setting[b]	Core	Rim	Core	Rim	Core	Rim	Core	Mantle	Rim	OR
wt%										
SiO_2	35.93	35.43	48.55	48.27	58.99	59.09	37.46	37.52	37.76	37.74
TiO_2	5.36	5.54	0.03	0.02	0.00	0.02	0.02	0.03	0.00	0.00
Al_2O_3	16.07	15.96	32.06	31.95	25.71	26.00	21.18	21.19	21.40	21.58
Cr_2O_3	0.00	0.00	0.00	0.00	0.00	0.00	0.00	0.00	0.00	0.00
FeO	16.92	16.17	6.40	6.29	0.08	0.13	30.68	31.06	31.69	30.97
MnO	0.03	0.03	0.09	0.09	0.00	0.05	0.96	1.08	1.05	1.03
MgO	11.98	11.60	9.87	9.99	0.02	0.00	7.69	7.75	7.47	7.42
ZnO	0.03	0.08	0.00	0.00	0.08	0.01	0.03	0.00	0.00	0.00
CaO	0.03	0.04	0.05	0.03	7.59	7.62	1.36	1.43	1.30	1.33
Na_2O	0.09	0.15	0.07	0.10	6.96	6.97	0.01	0.00	0.02	0.00
K_2O	9.54	9.53	0.00	0.02	0.24	0.22	0.00	0.00	0.00	0.02
Total[c]	95.98	94.53	97.14	96.77	99.67	100.11	99.38	100.06	100.69	100.09
Oxygen	11	11	18	18	8	8	12	12	12	12
Si	2.69	2.69	5.01	4.99	2.65	2.64	2.94	2.93	2.93	2.95
Ti	0.30	0.32	0.00	0.00	0.00	0.00	0.00	0.00	0.00	0.00
Al	1.42	1.43	3.90	3.89	1.36	1.37	1.96	1.95	1.96	1.99
Cr	0.00	0.00	0.00	0.00	0.00	0.00	0.00	0.00	0.00	0.00
Fe^{3+}[d]	0.05	0.05	0.10	0.15	0.00	0.00	0.15	0.19	0.17	0.12
Fe^{2+}	1.01	0.98	0.45	0.39	0.00	0.00	1.86	1.84	1.89	1.90
Mn^{2+}	0.00	0.00	0.01	0.01	0.00	0.00	0.06	0.07	0.07	0.07
Mg	1.34	1.31	1.52	1.54	0.00	0.00	0.90	0.90	0.87	0.86
Zn	0.00	0.00	0.00	0.00	0.00	0.00	0.00	0.00	0.00	0.00
Ca	0.00	0.00	0.01	0.00	0.36	0.36	0.11	0.12	0.11	0.11
Na	0.01	0.02	0.01	0.02	0.61	0.60	0.00	0.00	0.00	0.00
K	0.91	0.92	0.00	0.00	0.01	0.01	0.00	0.00	0.00	0.00
Total	7.73	7.73	11.00	11.00	5.00	5.00	8.00	8.00	8.00	8.00
Compositional variables										
XFe[e]	0.43	0.43	0.23	0.20	–	–	0.67	0.67	0.69	0.69

NOTES: –, not applicable
(a) Mineral abbreviations explained in the caption to Figure 2
(b) OR, outer rim
(c) Totals on anhydrous basis
(d) Fe^{3+} contents for biotite assumed to be 10% of Fe total; Fe^{3+} contents for other minerals based on Droop (1987)
(e) XFe = $Fe^{2+}/(Fe^{2+} + Mg)$

Table 3. Measured whole-rock and modelled compositions for sample 198585: pelitic gneiss, Griffins Find

XRF whole-rock composition (wt%)[a]

SiO_2	**TiO_2**	**Al_2O_3**	**Fe_2O_3**[b]	**FeO**[b]	**MnO**	**MgO**	**CaO**	**Na_2O**	**K_2O**	**P_2O_5**	**LOI**	**Total**
54.48	0.94	17.88	0.34	12.7	0.18	7.60	1.38	0.47	1.48	0.08	0.61	98.14

Normalized composition used for phase equilibria modelling (mol%)

SiO_2	**TiO_2**	**Al_2O_3**	**O**[c]	**FeO^T**[d]	**MnO**	**MgO**	**CaO**[e]	**Na_2O**	**K_2O**	**--**	**H_2O**[f]	**Total**
58.59	0.76	11.33	0.13	11.68	0.16	12.18	1.47	0.49	1.02	--	2.19	100

NOTES: (a) Data and analytical details are available from the WACHEM database <http://geochem.dmp.wa.gov.au/geochem/>
(b) FeO analysed by Fe^{2+} titration; Fe_2O_3 content calculated by difference
(c) O content (for Fe_2O_3) derived from the titration value
(d) FeO^T = moles FeO + 2 * moles O
(e) CaO modified to remove apatite: CaO(Mod) = CaO(Total) - (moles CaO(in Ap) = 3.33 * moles P_2O_5)
(f) H_2O content is the measured LOI

Results

Metamorphic *P–T* estimates have been derived based on detailed examination of one thin section and the bulk rock composition; care was taken to ensure that the thin section and the sample volume selected for whole-rock chemistry were similar in terms of featuring the same minerals in approximately the same abundances (Table 1), to minimize any potential compositional differences. The *P–T* pseudosection was calculated over a *P–T* range of 2–8 kbar and 550–950 °C (Fig. 3). The solidus is located between 710 and 850 °C across the range of modelled pressures. Cordierite is stable across the range of modelled temperatures, with a maximum pressure of 7.7 kbar at 715 °C. Orthopyroxene is stable below 7.9 kbar at 550 °C, 4.3 kbar at 585 °C, and 6.3 kbar at 895 °C. K-feldspar is stable above 615 °C and below 845 °C at 2 kbar and above 780 °C and below 920 °C at 5.7 kbar. Rutile is stable above 4.5 kbar at 550 °C and up to higher pressures at higher temperatures across the range of modelled conditions.

Metamorphic *P–T* estimates (± 2σ uncertainty) calculated using multiple-reaction thermobarometry are 5.2 ± 0.5 kbar and 833 ± 42 °C (Goscombe et al., 2019). These calculations used the core compositions (Table 2) to estimate peak conditions.

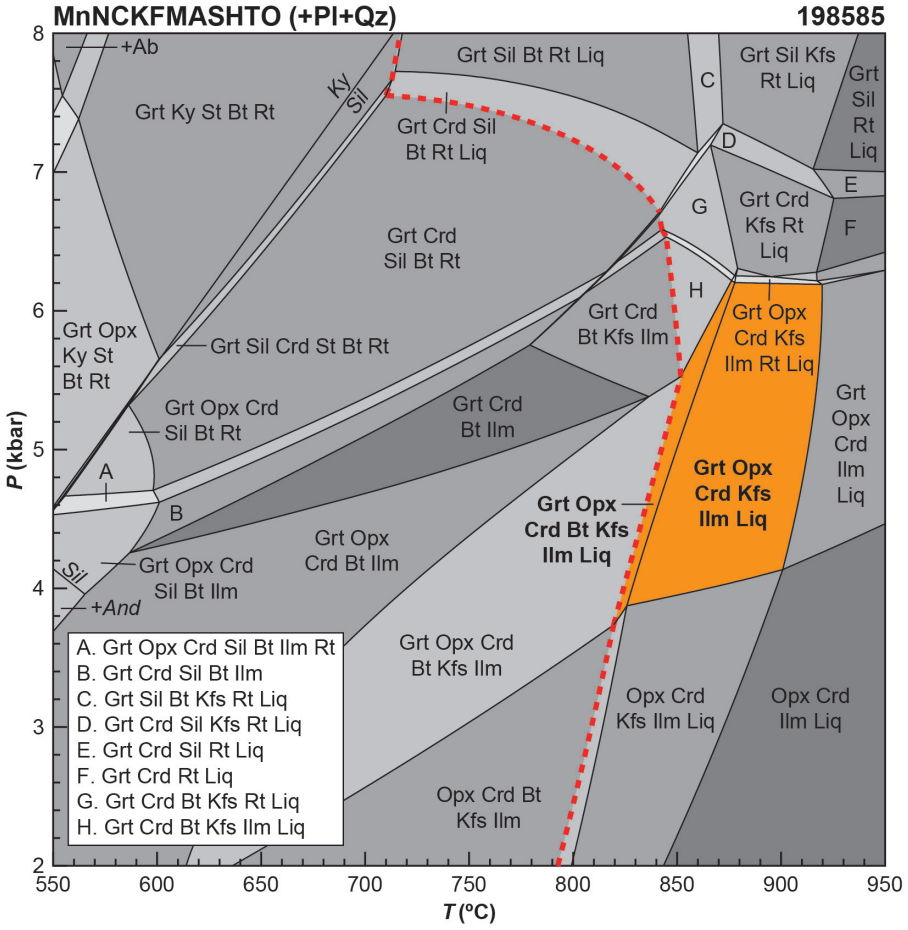

Figure 3. ***P–T*** **pseudosection calculated for sample 198585: pelitic gneiss, Griffins Find. Assemblage fields corresponding to peak metamorphic conditions are delimited by bold text and orange shading. Red dashed line represents the solidus. Abbreviations: And, andalusite; Bt, biotite; Crd, cordierite; Grt, garnet; Ilm, ilmenite; Kfs, K-feldspar; Ky, kyanite; Liq, silicate melt; Opx, orthopyroxene; Pl, plagioclase; Qz, quartz; Rt, rutile; Sil, sillimanite; St, staurolite**

Interpretation

Based on the coarser grain size and mineral associations that support textural equilibrium, the peak granulite-grade metamorphic assemblage is interpreted to be garnet–orthopyroxene–cordierite–plagioclase–quartz–ilmenite–melt(–biotite–K-feldspar). The rims of garnet porphyroblasts are inferred to be part of the peak metamorphic assemblage, and the growth of the cores occurred during prograde metamorphism. Biotite rims on garnet porphyroblasts are interpreted to post-date garnet growth, although some biotite that is intergrown with orthopyroxene, cordierite and quartz could have been part of the peak metamorphic assemblage. Cordierite in the matrix is interpreted to have been stable during peak- to post-peak metamorphism. Cordierite and orthopyroxene are generally in textural equilibrium, although in some portions of the thin section the relative sequence of growth is ambiguous. This ambiguity suggests that some domains may have promoted cordierite growth at the expense of orthopyroxene, whereas other domains promoted orthopyroxene growth at the expense of cordierite, supporting the interpretation that the growth of cordierite and orthopyroxene was broadly synchronous during peak- to post-peak metamorphism.

The inferred peak assemblage comprises garnet–orthopyroxene–cordierite–plagioclase–quartz–ilmenite–melt(–biotite–K-feldspar). There is uncertainty on whether biotite is part of the peak assemblage or a retrograde phase. The peak assemblage of garnet–orthopyroxene–cordierite–biotite–K-feldspar–plagioclase–quartz–ilmenite–melt is stable between 820 and 875 °C at 3.7 – 6.2 kbar. The biotite-absent field is stable at slightly higher temperatures of 825–920 °C, at similar pressures. Both fields are limited at lower pressure by the loss of garnet, the growth of rutile at higher pressure and loss of K-feldspar at higher temperatures. The predicted mineral modes (molar proportions approximately equivalent to vol%) within the peak field at 890 °C are broadly similar to the modes observed in the thin section (Table 1). The amount of biotite preserved in the thin section (= 15%) is similar to the predicted mode of melt in the peak field (16–18%; Table 1), supporting the interpretation that the retrograde growth of biotite was related to melt crystallization. A small amount of K-feldspar is predicted in the modelling (Fig. 4a; Table 1), although no K-feldspar was observed in thin section. Cordierite and orthopyroxene have relatively shallow modal isopleths across the peak field, and increase in modal proportion with a decrease in pressure at the expense of garnet (Fig. 4b–d).

Peak metamorphic conditions are estimated at 820–920 °C and 3.7 – 6.2 kbar, with an apparent thermal gradient between 140 and 215 °C/kbar. Mineral compositions are consistent with equilibration at 833 ± 42 °C, 5.2 ± 0.5 kbar, corresponding to an apparent thermal between 140 and 180 °C/kbar. There is little information on the prograde *P–T* path, but the growth of cordierite and orthopyroxene at the expense of garnet supports a decrease in pressure following peak metamorphism, with subsequent cooling to the solidus and growth of retrograde biotite, suggestive of a clockwise retrograde trajectory.

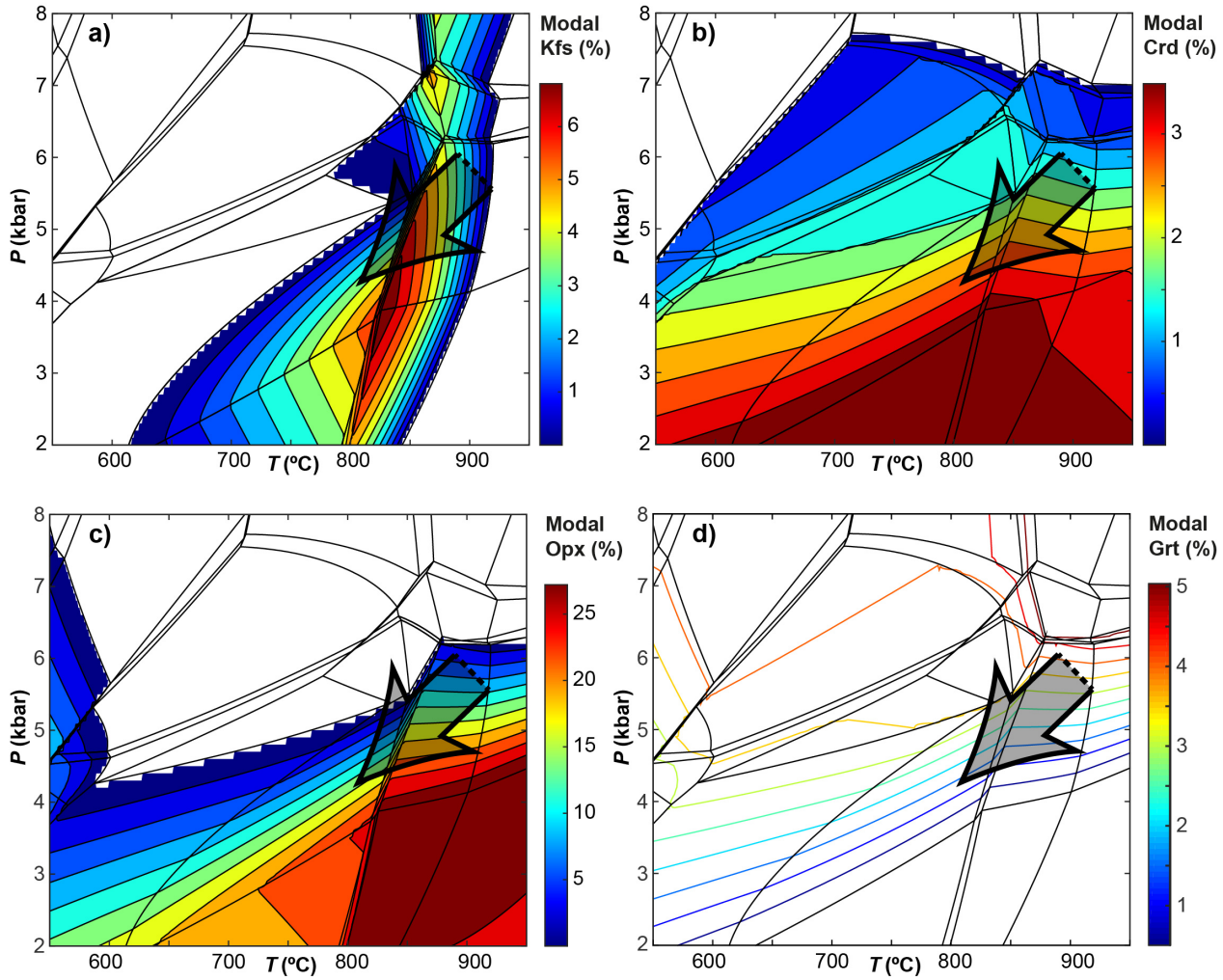

Figure 4. **Mode isopleths (mineral proportions; approximately equal to volume percent) for selected minerals in sample 198585.1: pelitic gneiss, Griffins Find (see Figure 3 for labelled *P–T* diagram). The growth of cordierite and orthopyroxene at the expense of garnet occurred with a decrease in pressure following peak metamorphism; schematic post-peak *P–T* path is represented by the grey arrow, with thickness of the arrow to qualitatively depict uncertainty**

References

Droop, GTR 1987, A general equation for estimating Fe^{3+} concentrations in ferromagnesian silicates and oxides from microprobe analyses, using stoichiometric criteria: Mineralogical Magazine, v. 51, no. 361, p. 431–435.

Fielding, IOH, Wingate, MTD, Korhonen, FJ and Rankenburg, K 2021, 198585: pelitic gneiss, Griffins Find; Geochronology Record 1767: Geological Survey of Western Australia, 5p.

Goscombe, B, Foster, DA, Blewett, R, Czarnota, K, Wade, B, Groenewald, B and Gray, D 2019, Neoarchaean metamorphic evolution of the Yilgarn Craton: a record of subduction, accretion, extension and lithospheric delamination: Precambrian Research, article no. 105441, doi:10.1016/j.precamres.2019.105441.

Holland, TJB and Powell, R 1998, An internally consistent thermodynamic data set for phases of petrological interest: Journal of Metamorphic Geology, v. 16, no. 3, p. 309–343.

Holland, TJB and Powell, R 2011, An improved and extended internally consistent thermodynamic dataset for phases of petrological interest, involving a new equation of state for solids: Journal of Metamorphic Geology, v. 29, no. 3, p. 333–383.

Korhonen, FJ, Kelsey, DE, Fielding, IOH and Romano, SS 2020, The utility of the metamorphic rock record: constraining the pressure–temperature–time conditions of metamorphism: Geological Survey of Western Australia, Record 2020/14, 24p.

Lu, Y, Wingate, MTD, Kirkland, CL, Goscombe, B and Wyche, S 2015a, 198578: pelitic gneiss, Griffins Find; Geochronology Record 1284: Geological Survey of Western Australia, 4p.

Lu, Y, Wingate, MTD, Kirkland, CL, Goscombe, B and Wyche, S 2015b, 198580: quartzite, Griffins Find; Geochronology Record 1285: Geological Survey of Western Australia, 5p.

Pearce, MA, White, AJR and Gazley, MF 2015, TCInvestigator: automated calculation of mineral mode and composition contours for thermocalc pseudosections: Journal of Metamorphic Geology, v. 33, no. 4, p. 413–425, doi:10.1111/jmg.12126.

Pidgeon, RT, Wingate, MTD, Bodorkos, S and Nelson, DR 2010, The age distribution of detrital zircons in quartzites from the Toodyay – Lake Grace Domain, Western Australia: implications for the early evolution of the Yilgarn Craton: American Journal of Science, v. 310, p. 1115–1135.

Powell, R and Holland, TJB 1988, An internally consistent dataset with uncertainties and correlations: 3. Applications to geobarometry, worked examples and a computer program: Journal of Metamorphic Geology, v. 6, no. 2, p. 173–204.

Qiu, Y and McNaughton, NJ 1999, Source of Pb in orogenic lode-gold mineralisation: Pb isotope constraints from deep crustal rocks from the southwestern Archaean Yilgarn Craton, Australia: Mineralium Deposita, v. 34, p. 366–381.

Quentin de Gromard, R, Ivanic, TJ and Zibra, I 2021, Interpreted bedrock geology of the southwest Yilgarn Craton, Geological Survey of Western Australia, in press.

White, RW, Powell, R, Holland, TJB, Johnson, TE and Green, ECR 2014a, New mineral activity-composition relations for thermodynamic calculations in metapelitic systems: Journal of Metamorphic Geology, v. 32, no. 3, p. 261–286.

White, RW, Powell, R and Johnson, TE 2014b, The effect of Mn on mineral stability in metapelites revisited: New a-x relations for manganese-bearing minerals: Journal of Metamorphic Geology, doi:10.1111/jmg.12095.

Wilde, SA 2001, Jimperding and Chittering metamorphic belts, Western Australia— a field guide: Geological Survey of Western Australia, Record 2001/12, 24p.

Links

Metamorphic history introduction document: Intro_2020.pdf

Appendix

Quantitative EPMA compositional maps for sample 198585: pelitic gneiss, Griffins Find, calculated for proportion of garnet end-members. The analysed garnet grain is identified in Figure 1

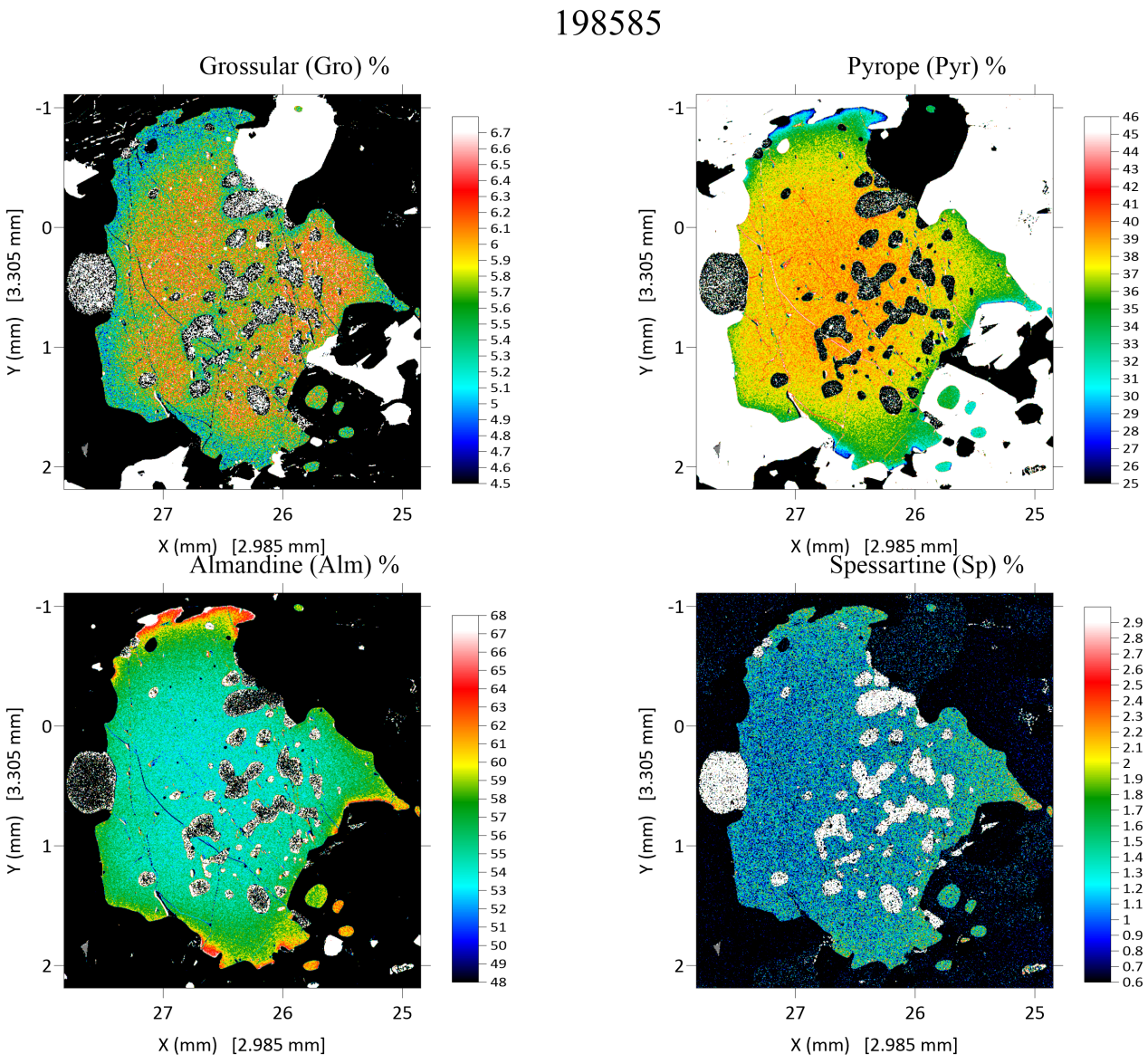

Recommended reference for this publication

Blereau, ER, Korhonen, FJ, Fielding, IOH, Romano, SS, Kelsey, DE and Roberts, MP 2021, 198585: pelitic gneiss, South West Terrane; Metamorphic History Record 1: Geological Survey of Western Australia, 9p.

This Metamorphic History Record was last modified on 9 June 2021.

Grid references in this publication refer to the Geocentric Datum of Australia 1994 (GDA94). All locations are quoted to at least the nearest 100 m.

WAROX is GSWA's field observation and sample database. WAROX site IDs have the format 'ABCXXXnnnnnnSS', where ABC = geologist username, XXX = project or map code, nnnnnn = 6 digit site number, and SS = optional alphabetic suffix (maximum 2 characters).

Isotope and element analyses are routinely conducted using the GeoHistory laser ablation ICP-MS and Sensitive High-Resolution Ion Microprobe (SHRIMP) ion microprobe facilities at the John de Laeter Centre (JdLC), Curtin University, with the financial support of the Australian Research Council and AuScope National Collaborative Research Infrastructure Strategy (NCRIS). The TESCAN Integrated Mineral Analyser (TIMA) instrument was funded by a grant from the Australian Research Council (LE140100150) and is operated by the JdLC with the support of the Geological Survey of Western Australia, The University of Western Australia (UWA) and Murdoch University. Mineral analyses are routinely obtained using the electron probe microanalyser (EPMA) facilities at the Centre for Microscopy, Characterisation and Analysis at UWA, and at Adelaide Microscopy, University of Adelaide.

Digital data related to WA Geology Online, including geochronology and digital geology, are available online at the Department's Data and Software Centre and may be viewed in map context at GeoVIEW.WA.

Disclaimer
This product uses information from various sources. The Department of Mines, Industry Regulation and Safety (DMIRS) and the State cannot guarantee the accuracy, currency or completeness of the information. Neither the department nor the State of Western Australia nor any employee or agent of the department shall be responsible or liable for any loss, damage or injury arising from the use of or reliance on any information, data or advice (including incomplete, out of date, incorrect, inaccurate or misleading information, data or advice) expressed or implied in, or coming from, this publication or incorporated into it by reference, by any person whosoever.

© State of Western Australia (Department of Mines, Industry Regulation and Safety) 2021

With the exception of the Western Australian Coat of Arms and other logos, and where otherwise noted, these data are provided under a Creative Commons Attribution 4.0 International Licence. (http://creativecommons.org/licenses/by/4.0/legalcode)

Further details of geoscience products are available from:
Information Centre
Department of Mines, Industry Regulation and Safety
100 Plain Street
EAST PERTH WA 6004
Telephone: +61 8 9222 3459 | Email: publications@dmirs.wa.gov.au
www.dmirs.wa.gov.au/GSWApublications